

TESTING THE ISOTROPY OF THE HUBBLE EXPANSION

K. Migkas,¹ M. Plionis^{2,3,4}

Draft version: May 31, 2021

RESUMEN

Hemos utilizado la compilación *Union2.1* de SNIa para buscar posibles anisotropías de la expansión de Hubble, dividiendo el cielo en 9 ángulos sólidos que contienen más o menos el mismo número de SNIa, así como en los dos hemisferios galácticos. Como resultado se identificó una región del cielo que contiene 82 SNIa (15% del total con $z > 0.02$) y que parece tener un comportamiento de expansión Hubble significativamente diferente de resto de la muestra. Pero la cause es un efecto sistemático relacionado mayormente al comportamiento “errático” de solo tres SNIa. Además, el análisis por separado del los dos hemisferios galácticos resulta en diferentes parámetros cosmológicos, pero que todavía no es lo suficientemente significativo para afirmar la detección de una anisotropía de la expansión Hubble. Llegamos a la conclusión de que incluyendo en el análisis unos pocos SNIa con valores atípicos puede proporcionar indicaciones artificiales de anisotropías.

ABSTRACT

We have used the *Union2.1* SNIa compilation to search for possible Hubble expansion anisotropies, dividing the sky in 9 solid angles containing roughly the same number of SNIa, as well as in the two Galactic hemispheres. We identified only one sky region, containing 82 SNIa ($\sim 15\%$ of total sample with $z > 0.02$), that indeed appears to share a significantly different Hubble expansion than the rest of the sample. However, this behaviour appears to be attributed to the joint “erratic” behaviour of only three SNIa and not to an anisotropic expansion. We also find that the northern and southern galactic hemispheres have different cosmological parameter solutions but still not significant enough to assert the detection of a Hubble expansion anisotropy. We conclude that even a few outliers can have such an effect as to induce artificial indications of anisotropies, when the number of analysed SNIa is relatively small.

Key Words: (cosmology:) Cosmological parameters — supernovae: general — methods: statistical

¹Argelander Institute for Astronomy (AIfA), University of Bonn, Auf dem Hugel 71, 53121 Bonn, Germany

²Astrophysics, Astronomy & Mechanics Sector, Physics Department, Aristotle University of Thessaloniki, 54124 Greece

³IAASARS, National Observatory of Athens, 11810 Greece

⁴Instituto Nacional de Astrofísica, Óptica y Electrónica, Puebla, México C.P. 72840

1. INTRODUCTION

The isotropy and homogeneity of the Universe, the principle on which the Friedmann-Robertson-Walker cosmological models are based, is strongly supported by several observational data, among which the isotropy of the Cosmic Microwave Background (CMB) radiation (eg., Ade et al. 2014), the large scale distribution of radio sources (Wu, Lahav & Rees 1999) and the Hubble expansion as traced by supernovae type Ia (SNIa) (eg., Riess et al. 1998, Perlmutter et al. 1999, Suzuki et al. 2012, Betoule et al. 2014).

The SNIa are excellent cosmological probes of the Hubble expansion up to high redshifts ($z \leq 1.7$) due to the fact that they are considered as "standard candles" (Kowal 1968, Barbon et al. 1973, Riess et al. 1998, Perlmutter et al. 1999), once the so-called "stretch" and color corrections have been applied. These corrections are necessary because the SNIa peak brightness correlates with their color, the light-curve width and the mass of the host galaxy (see Kowalski et al. 2008, Amanullah et al. 2010, Suzuki et al. 2012, Betoule et al. 2014). Other high- z tracers of the Hubble expansion have been proposed, such as HII galaxies (Melnick, Terlevich & Terlevich 2000; Plionis et al. 2011) and GRB's (Ghirlanda et al. 2006). Such cosmic tracers can be used to test the Cosmological Principle by confirming or not the isotropy of the Hubble expansion. Several recent studies have focused in this subject, among which those of Kolatt & Lahav (2001), Bonvin, Durrer & Kunz (2006), Schwarz & Weinhorst (2007), Blomqvist, Moertsell & Nobili (2008), Gupta, & Saini (2010), Cooke & Lynden-Bell (2010), Antoniou & Perivolaropoulos (2010), Mariano & Perivolaropoulos (2012), Kalus et al. (2013), Yang, Wang & Chu (2013), Heneka, Marra & Amendola (2014), Javanmardi et al. (2015). It is interesting to note that various of the previously mentioned studies have found a low-significance dipole correlated with the general direction of the CMB dipole.

In this work we use the *Union2.1* sample in order to search for possible anisotropies of the Hubble expansion. The approach that we follow is to attempt to identify solid angles that show a different expansion behaviour with respect to the rest. In our analysis we use only those SNIa with redshifts $z \geq 0.02$ in order to avoid uncertainties in their estimated distances due to the local bulk flows (eg., Ma & Pan 2014; Appleby, Shafieloo & Johnson 2015).

2. DATA AND METHODOLOGY

2.1. *Union2.1* SNIa sample

The *Union2.1* is one of the largest compilations of supernovae of type Ia (Suzuki et al. 2012). It originally consisted of 833 SNe drawn from 19 different datasets, but after a variety of homogenization selection criteria (eg. lightcurve quality cuts) 580 remained, out of which 546 SNIa with $z \geq 0.02$ and 29 with $z > 1$. The high-redshift SNIa are extremely important in calculating the cosmological parameters, because the differences of various Dark Energy

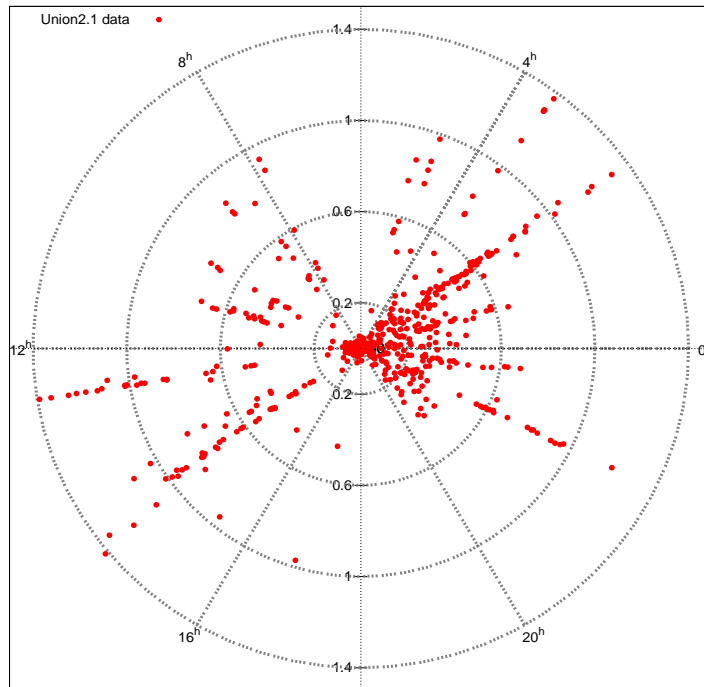


Fig. 1. Pie diagram of the 580 SNIa of the *Union2.1* set.

(DE hereafter) models are larger and more significant at such redshifts (for example see Fig.1 in Plionis et al. 2011).

We note that the final *Union2.1* SNIa distance moduli provided and used in the current paper have been obtained by assuming a common, independent of their direction, correction for the “stretch”, color and host-galaxy parameters for all SNIa (Suzuki et al. 2012).

In order to visualize the angular and redshift distribution of the *Union2.1* SNIa sample, we produce a pie diagram with the redshift, z , being the radius and the right ascension, α , being the angle (Fig. 1). As we can see the higher- z SNIa are detected preferentially along specific directions, some of which contain more data than others. This non uniform distribution of data, in terms of coordinates, is a result of the fact that the observational campaigns cover very small solid angles of the sky.

2.2. Quantifying the Hubble flow

The basic procedure by which the Hubble expansion is traced observationally is through the so-called distance modulus, μ , defined by:

$$\mu = m - M = 5 \log d_L + 25 \quad (1)$$

where m and M are the apparent and absolute magnitude of the SNIa, and d_L its luminosity distance, given for a flat geometry ($\Omega_k = 0$) by:

$$d_L = c(1+z) \int_0^z \frac{dx}{H(x)}. \quad (2)$$

with $H(z)$ the so-called Hubble parameter, defined using the 1st Friedmann equation, by:

$$H(z) = H_0 \sqrt{\Omega_{m,0}(1+z)^3 + \Omega_{k,0}(1+z)^2 + \Omega_\Lambda \exp\left(3 \int_0^z \frac{1+w(x)}{1+x} dx\right)} \quad (3)$$

with H_0 the Hubble constant and $\Omega_{m,0}$, $\Omega_{k,0}$, Ω_Λ the fractional densities of matter, curvature and the cosmological constant or DE respectively at the present epoch, while w is the equation of state parameter of Dark Energy. It is evident that the luminosity distance depends strongly on the cosmological parameters. Different DE models reflect to the functional form of the $w(x)$. The QDE model (Quintessence DE), that we will use in the current study, assumes a constant equation of state parameter, w , that can admit values different than -1 .

The assumption of the isotropic Hubble expansion boils down in having a Hubble parameter $H(z)$ being a function only of z and not of direction. Therefore, different radial directions should provide statistically equivalent $H(z)$. The approach we use in this analysis is exactly to investigate different radial directions, or solid angles, in order to confirm or not the independence of $H(z)$ on direction. The criterion of equivalence in the Hubble expansion among the different solid angles will be whether the resulting cosmological parameters, $(\Omega_{m,0}, w)$, provided by fitting the data to the above Hubble expansion models, are statistically consistent among them and among the solution using the whole ($z > 0.02$) *Union2.1* compilation.

2.3. The χ^2 -minimization procedure

In order to fit the cosmological parameters of eq.(3) we minimize the difference between the SNIa observed distance moduli and the theoretical ones via eq.(1). To this end we use a χ^2 minimization procedure outlined below.

Suppose we have a measurement of the distance modulus $\mu_{obs}(z_i)$ with uncertainty σ_μ , which comes with its redshift z_i . The theoretically expected distance modulus for the same redshift z_i is $\mu_{th}(z_i, \mathbf{p})$, with $\mathbf{p} \equiv w, \Omega_{m,0}$ being the model's free parameters. Now suppose that we have N $\mu_{obs}(z_i)$ independent measurements. The total probability of obtaining this entire set of these N data points is equal to the product of the probability of each data point, so :

$$P_{\text{tot}} = \prod_{i=1}^N P(z_i) = \left[\prod_{i=1}^N \frac{1}{\sigma_i \sqrt{2\pi}} \right] \exp \left[-\frac{1}{2} \sum_{i=1}^N \left(\frac{\mu_{obs}(z_i) - \mu_{th}(z_i, \mathbf{p})}{\sigma_i} \right)^2 \right] \quad (4)$$

If we want to find the maximum probability we have to minimize the sum in the exponential term of P_{tot} , and therefore, this quantity is defined as:

$$\chi^2 = \sum_{i=1}^N \left(\frac{\mu_{\text{obs}}(z_i) - \mu_{\text{th}}(z_i, \mathbf{p})}{\sigma_i} \right)^2 \quad (5)$$

the minimum value of which, χ_{min}^2 , provides the maximum probability of P_{tot} . Thus, since the theoretical expected $\mu_{\text{th}}(z_i, \mathbf{p})$, depend on a set of free parameters, which correspond to the elements of the vector \mathbf{p} [in our case $\mathbf{p} = (\Omega_{m,0}, w)$], we can test for which values of these parameters we get the maximum probability. In our current analysis we ignore the covariance matrix of the errors in the observed SNIa distance moduli and use the root-mean-square of the diagonal elements, provided with the *Union2.1* catalogue. Also, we use the approach of Nesseris & Perivolaropoulos (2006) by which we do not need to impose an *a priori* value of the Hubble constant.

The best fit value of the free parameters, \mathbf{p}_0 , are provided for the χ_{min}^2 . When the parameters differ from these values, $\mathbf{p} \neq \mathbf{p}_0$, then the χ^2 increases, so $\Delta\chi^2 = \chi^2 - \chi_{\text{min}}^2 > 0$. Limits of $\Delta\chi^2$ that depend on the number of the fitted parameters N_f , define confidence regions that contain a certain fraction of the probability distribution of \mathbf{p} 's. For our case of $N_f = 2$, the 1, 2 and 3 σ confidence regions correspond to $\Delta\chi^2 = 2.3, 6.17$ and 11.83, respectively.

3. RESULTS

Using the whole ($z > 0.02$) *Union2.1* sample we derive, as expected, the already published QDE model constrains of:

$$\Omega_{m,0} = 0.282 \pm 0.03 \quad \text{and} \quad w = -1.013 \pm 0.083 \quad \text{with} \quad \chi^2/dof = 0.9567 \quad (6)$$

fully consistent with those of Suzuki et al. (2012). Now, we proceed with the main scope of our work which is to identify possible anisotropies of the Hubble flow.

3.1. Dividing the sky into 9 solid angles

As a first test we divide the celestial sphere in nine fully independent solid angles, shown in Figure 2, so that each has a similar number of SNIa. We then fit the QDE cosmological parameters in each, by using the previously described minimization procedure. Doing so, we identified one sky region with a distinctly different $\Omega_{m,0} - w$ solution with respect to all other regions of the sky as well as with respect to the whole *Union2.1* sample together. This region, which we call Group X, contains 82 SNIa and has galactic coordinates within: $35^\circ < l < 83^\circ$ and $-79^\circ < b < -37^\circ$ (delineated within thick lines in Figure 2). We have verified that the SNIa redshift distribution in this region does not present any ‘‘peculiarity’’ with respect to the overall. In fact, although the redshift distributions of the separate regions show different levels of consistency with the overall *Union2.1* redshift distribution,

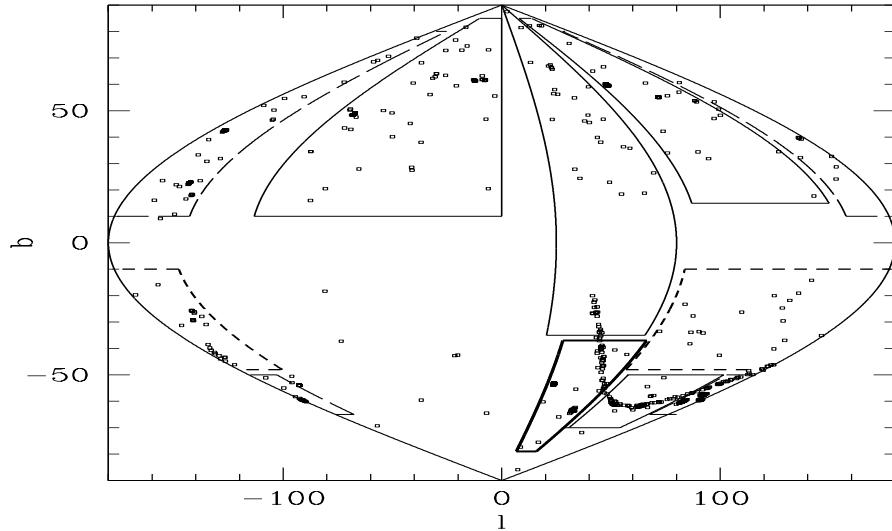


Fig. 2. The celestial sphere in equal area projection with 8 separate regions delineated (the 9th region is the rest of the sky). The area delineated with thick lines corresponds to Group-X. Dashed lines are used when a region folds over into the Galactic longitude direction.

the Kolmogorov-Smirnov significance of which vary from $\mathcal{P} \sim 10^{-7}$ up to ~ 0.13 , that of the Group X is the most statistically consistent with the overall ($\mathcal{P} \simeq 0.13$). Thus a “peculiar” redshift distribution is not the cause of the Group X’s $\Omega_{m,0} - w$ solution behaviour.

In the left panel of Figure 3 we compare the 1σ contour region of Group X with that of the rest of the *Union2.1* sample and as it can be seen their respective 1σ contour regions have no common area, indicating a relatively significant difference. Quantitatively, the difference of the latter best-fit solution with respect to that of Group X is of $\Delta\chi^2 \simeq 4.3$ (ie., the probability of being different is $\sim 90\%$).

In order to visualise the uniqueness of the Group X behaviour we plot in the right panel of Figure 3 the fraction of the QDE 1σ contour area, based on the whole *Union2.1* (excluding the Group X), which is common with that based on every one of the 9 independent subsamples of SNIa. We observe that the 1σ solution space of the entire sample is fully (100%) encompassed within almost each of the other 8 subsamples (with one exception which is at 60%; the corresponding region is delineated with short-dashed lines in Figure 2), besides Group X which is at 0%.

It is interesting to note that Group X is near the CMB dipole anti-apex direction. Furthermore, many studies have consistently been finding the largest deviations from an isotropic expansion occurring near this direction. For example, as early as 2001 and using only 79 SNIa, Kolatt & Lahav (2001) found a Hubble diagram dipole pointing towards $(l, b) \simeq (80^\circ, -20^\circ)$. Antoniou &

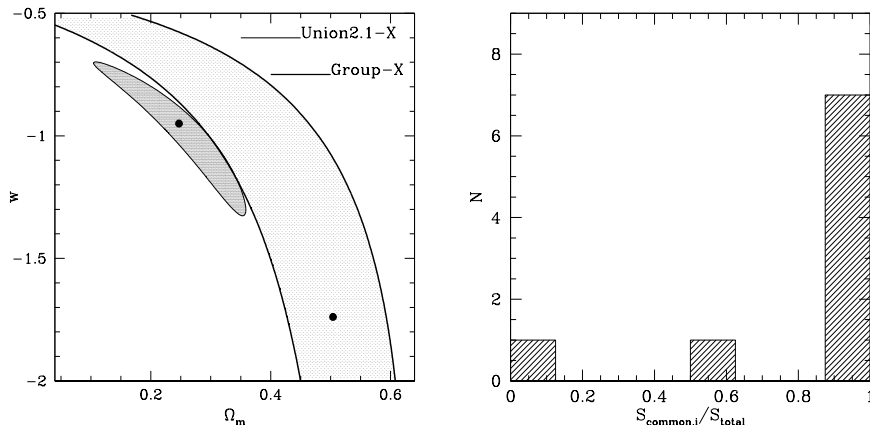


Fig. 3. *Left panel:* 1σ contour plots of Group X (thick contour and light greyscale, 82 SNIa) and for the rest of the *Union2.1* data (thin contour and dark greyscale, 464 SNIa). *Right panel:* Distribution of the common 1σ contour area (between each of the 9 individual subsamples and the whole SNIa sample) divided by the 1σ area of the entire sample.

Perivolaropoulos (2010) using the *Union2* SNIa sample and separately Cooke & Lynden-Bell (2010), using the slightly earlier *Union* sample, also found a preferred axis of minimum acceleration in the same general direction but at a low significance level. Yang, Wang & Chu (2013) using the *Union2.1* SNIa data also found a low significance preferred direction of the accelerating expansion. Finally, Javanmardi et al. (2015), found as the most discrepant direction of the Hubble expansion that centered on $(l, b) \simeq (67.5^\circ, -66.4^\circ)$, which indeed coincides with our Group X.

3.2. Possible systematic effects

The statistically important “erratic” behaviour of Group X with respect to the rest of the SNIa could be due to a variety of reasons, among which an intrinsic anisotropy of the Hubble expansion, a large bulk flow in this part of the sky or some unknown systematic observational error (see for example Heneka et al. 2014). In this respect we remind the reader that the SNIa distance moduli, provided in the *Union2.1* compilation, have been derived assuming a global correction for individual deviations from the average SNIa light-curve and from the mean color. As highlighted in Javanmardi et al. (2015), the most robust approach for testing isotropy would be to find the values for the “stretch”, color and host-galaxy parameters for each patch of the sky separately. However, we adopt the simplified approach of the global correction, as in Javanmardi et al. (2015).

Below we present our analysis of two possible systematic observational effects that could be the cause of the “erratic” behaviour of Group X.

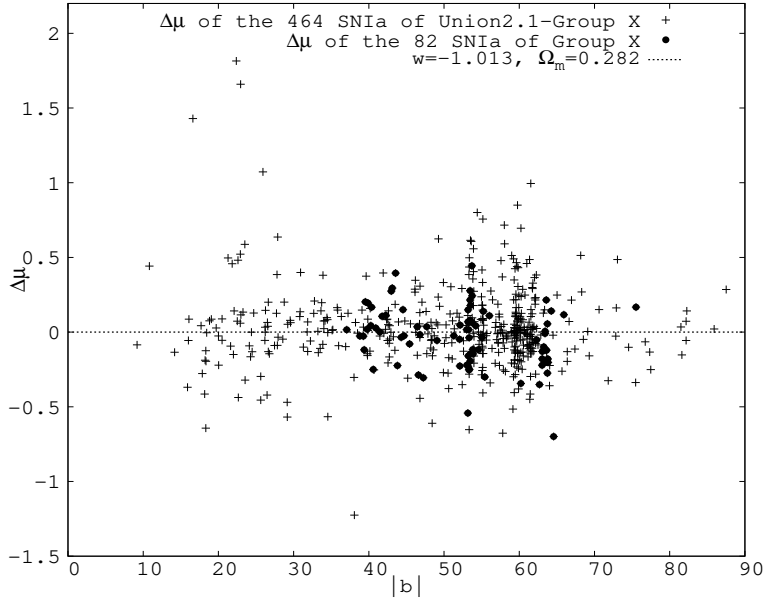


Fig. 4. Distance moduli deviation $\Delta\mu$, with respect to that of $(\Omega_{m,0}, w) = (0.282, -1.013)$, as a function of galactic latitude $|b|$ for the 546 *Union2.1* SNIa (crosses) and for the 82 SNIa of Group X (filled dots).

3.2.1. Galactic absorption

We test whether the erratic behaviour of Group X could be due to inadequately treating the Galactic absorption. To this end and for each SNIa we plot in Figure 4 the distance modulus deviation from that expected in the concordance model, i.e., $\Delta\mu = \mu_{obs}(z_i) - \mu_{th}(z_i, \mathbf{p})$ with $\mathbf{p} \equiv (w, \Omega_{m,0}) \equiv (-1.013, 0.282)$, as a function of the Galactic latitude $|b|$.

As it is illustrated in Figure 4, the SNIa distance moduli of Group X (in blue) do not show a distinct behaviour as a function of $|b|$. However, we see that the SNIa with the largest $\Delta\mu$'s, i.e., the apparently faintest ones, are all at small $|b|$'s, which strongly hints towards some at least SNIa having magnitudes not adequately corrected, or overcorrected, for Galactic absorption. These SNIa (*1997k* with $b = 16.6^\circ$, *1997l* with $b = 22.4^\circ$ and *1997o* with $b = 22.9^\circ$) are also among the nearest to the plane of the Galaxy.

3.2.2. SNIa Outliers ?

We have investigated the possibility whether an erratic behaviour of one or a few SNIa could cause the mentioned effect. To this end we systematically exclude, one by one, each of the SNIa of Group X and check whether the QDE 1σ contour area of the remaining Group X increases its consistency with the *Union2.1* solution (excluding the Group X). We find that although the large majority of the single SNIa do not have any major contribution to the erratic

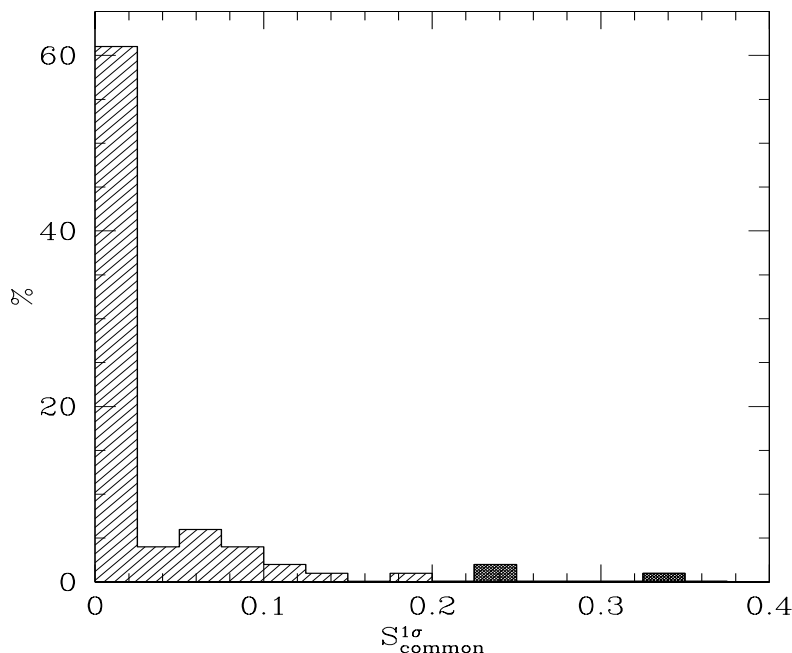


Fig. 5. Fraction of the *Union2.1* (excluding Group X) QDE 1σ solution area which is common with the corresponding area of Group X excluding one by one each Group X SNIa from the fitting procedure. Marked by dark shade are the three SNIa with the largest effect, the exclusion of which recovers the consistency of the Hubble expansion of Group X with that of the overall *Union2.1* sample.

behaviour of Group X, we do find that some individual SNIa have a very large effect on the Group X solution, as can be seen in Figure 5 where we plot the fraction of the overall *Union2.1* (excluding the Group X) 1σ contour area covered by the corresponding Group X 1σ contour area when excluding one SNIa at a time. The three cases that show a $> 20\%$ effect are shown in dark shade. The largest effect, that of a $\sim 35\%$ recovery of the common 1σ solution space, comes from excluding the *03D4cx* SNIa at $z = 0.949$. The next most important effect comes from *g050* at $z = 0.613$, which by excluding it results in a $\sim 25\%$ recovery of the common 1σ solution space, while the third most important effect, again at a $\sim 23\%$ level, comes from the *2005hv* at $z = 0.1776$. Most importantly, the joint effect of excluding all three “erratic” SNIa is the increase of the consistency from 0% to more than 93%, thus annulling the tension between the Group X and the rest of the *Union2.1* sample solution.

We conclude that the identified inconsistency of the Hubble expansion of the Group-X SNIa appears to be dominated by the erratic behaviour of only three out of the 82 SNIa, indicating the sensitivity of the Hubble expansion solution to outliers when small numbers of SNIa are investigated.

Excluding from the overall analysis the above three “erratic” SNIa as well

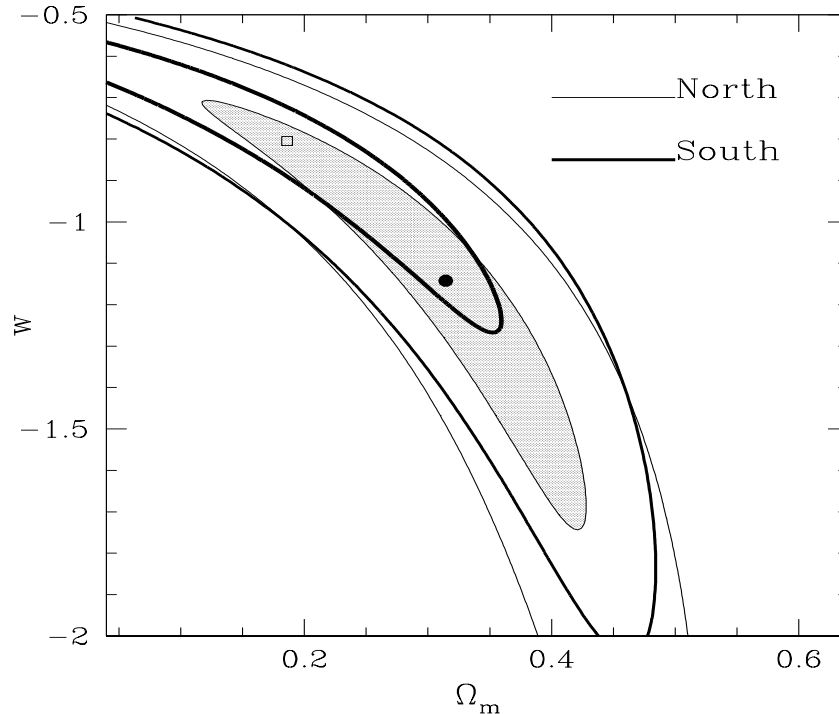


Fig. 6. The separate Galactic hemisphere solution: Thick lines correspond to the Southern G.H. while the greyscale to the Northern G.H. with their respective best fit values shown as empty and filled dots, respectively.

as the 3 SNIa at low galactic latitudes, which are suspect of an inadequate Galactic absorption correction, we find:

$$\Omega_{m,0} = 0.262^{+0.0313}_{-0.0296} \text{ and } w = -0.973 \pm 0.077 \text{ with } \chi^2/dof = 0.909 \quad (7)$$

Comparing with the solution using all the *Union2.1* set (eq. 6) we see a small but notable difference of the best fit $\Omega_{m,0}, w$ parameter values, while the χ^2/dof is also lower.

3.3. Separate Galactic hemispheres solutions

We now consider, as a final test of possible Hubble expansion anisotropies, the southern and northern Galactic hemispheres separately, excluding the 6 “erratic” SNIa identified previously. We therefore use 332 and 208 SNIa, respectively for the southern and northern hemisphere. The results are:

- South: $w = -0.805 \pm 0.084$, $\Omega_{m,0} = 0.186^{+0.0508}_{-0.0468}$, $\chi^2_{min}/dof = 0.9492$
- North: $w = -1.144^{+0.1325}_{-0.1440}$, $\Omega_{m,0} = 0.315^{+0.0405}_{-0.0377}$, $\chi^2_{min}/dof = 0.8500$

It can be seen that the best-fit QDE model parameters for the two hemispheres are quite different, with a $\Delta\chi^2 = 1.27$, but within the 1σ uncertainty contour range, as seen in Figure 6. Therefore this difference indicates some tension between the two hemisphere solution but does not appear to constitute evidence of a significant anisotropy.

4. CONCLUSIONS

We have searched for possible anisotropies of the Hubble expansion, using the *Union2.1* SNIa data. Our approach was to investigate separately the Hubble expansion traced by SNIa in 9 solid angles, covering the whole sky, as well as separately in the two Galactic hemispheres. We have identified only one particular sky region, with galactic coordinates $35^\circ < l < 83^\circ$ & $-79^\circ < b < -37^\circ$ (near the CMB dipole anti-apex direction), which provides a relatively significant different $\Omega_{m,0} - w$ solution with respect to the rest of the *Union2.1* compilation or any other subsample of similar size that we have analysed. Our investigation for the possible causes of this result has shown that probably it should not be attributed to an intrinsic anisotropy in the Hubble flow but rather on the erratic behaviour of only three SNIa, indicating the sensitivity of the measured Hubble expansion to outliers when relatively small numbers of SNIa are investigated. We have also found that the 3 most deviant SNIa distance moduli are located at very low-galactic latitudes, suggesting an inadequate Galactic absorption correction. Excluding the six problematic SNIa from the *Union2.1* sample results in a notable change the QDE model free parameters but not at a significant level. Finally, we have also found a quite different QDE parameters fit between the North and South Galactic hemispheres, but not significant enough to assert the detection of a Hubble expansion anisotropy.

REFERENCES

- Amanullah, R., Lidman, C., Rubin, D., et al. 2010, ApJ, **716**, 712
 Antoniou, A., Perivolaropoulos, L. 2010, JCAP, **12**, 012
 Appleby, S., Shafieloo, A. and Johnson, A. 2015, ApJ, **801**, 76
 Barbon, R., Ciatti, F., & Rosino, L. 1973, A&A, **25**, 241
 Betoule, M., Kessler, R., Guy, J., et al. 2014, A&A, **568**, 22
 Blomqvist, M., Mortsell, E., & Nobili, S. 2008, JCAP, **6**, 27
 Bonvin, C., Durrer, R., & Kunz, M. 2006, PRL, **96**, 191302
 Cooke, R., Lynden-Bell, D. 2010, MNRAS, **401**, 1409
 Ghirlanda, G., Ghisellini, G. and Firmani, C. 2006, NJPh, **8**, 123
 Gupta, S., & Saini, T. D. 2010, MNRAS, **407**, 651
 Heneka, C., Marra, V., & Amendola, L. 2014, MNRAS, **439**, 1855
 Javanmardi, B., Porciani, C., Kroupa, P., Pflamm-Altenburg, J. 2015, ApJ, **810**, 47
 Kolatt, T. S., Lahav, O. 2001, MNRAS, **323**, 859
 Kalus, B., Schwarz, D. J., Seikel, M., & Wiegand, A. 2013, A&A, **553**, A56
 Kowal, C. T. 1968, ApJ, **73**, 1021
 Kowalski, M., Rubin, D., Aldering, G., et al. 2008, ApJ, **686**, 749

- Ma, Y., & Pan, J. 2014, MNRAS, **437**, 1996
Mariano, A., Perivolaropoulos, L. 2012, PRD, **86**, 083517
Melnick, J., Terlevich, R., Terlevich, E. 2000, MNRAS, **311**, 629
Nesseris, S., Perivolaropoulos, L. 2006, PRD, **73**, 103511
Perlmutter, S., et al. 1999, ApJ, **517**, 565
Planck Collaboration (P. Ade *et. al.*) 2014, A&A, **571**, A1
Plionis, M., Terlevich, R., Basilakos, S., Bresolin, F., Terlevich, E., Melnick, J.,
Chavez, R. 2011, MNRAS, **416**, 2981
Riess, A. G., et al. 1998, AJ, **116**, 1009
Schwarz, D. J., & Weinhorst, B. 2007, A&A, **474**, 717
Suzuki N. et al. 2012, ApJ, **746**, 85
Wu, K. S., Lahav, O., & Rees, M. J. 1999, Nature, **397**, 225
Yang X. F., Wang F. Y., Chu Z. 2014, MNRAS, **437**, 1840

Full addresses go here